THE AMERICAN SOCIETY OF MECHANICAL ENGINEERS
Three Park Avenue, New York, N.Y. 10016-5990

99-GT-138

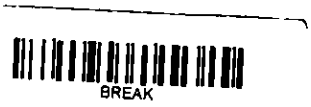

Assessing the Errors in Practical Gas Turbine Modelling

Ceri Evans and David Rees

University of Glamorgan, School of Electronics, Pontypridd, CF37 1DL, Wales, UK
Phone: +44 (0)1 443 482527 Fax: +44 (0)1 443 482541 E-mail: dcevans@glam.ac.uk

ABSTRACT

This paper deals with the three most important sources of error in the practical identification of linear gas turbine models. These are noise, nonlinearities and unmodelled linear dynamics. Techniques are described which allow each of these sources of error to be studied and their influence to be assessed.

NOMENCLATURE

F	Number of estimation frequencies.
FRF	Frequency response function.
NH	High Pressure (HP) shaft speed.
NL	Low Pressure (LP) shaft speed.
SNR	Signal-to-noise ratio.
T_D	Pure time delay.
$U(j\omega)$	Input Fourier coefficients.
$V(\mathbf{p})$	Estimator cost function.
V_{MIN}	Expected value of cost function.
W_f	Demanded fuel flow to burners.
$Y(j\omega)$	Output Fourier coefficients.
$\mathbf{i}$	Harmonic vector.
np	Number of estimation parameters.
$u(t)$	Input signal.
σ_p	Standard deviation of estimated poles.
σ_z	Standard deviation of estimated zeros.
ω_K	Angular frequency of the Kth harmonic.
γ_{nl}	Nonlinear coherence.
$(\bullet)^*$	Complex conjugate of $(\bullet)$.

1. INTRODUCTION

This paper examines the sources of error in the identification of linear gas turbine models from test data. The influence of each source of error is studied in turn.

A related paper was presented at the last ASME Gas Turbine Conference (Evans, 1998), which discussed the results of testing an aircraft gas turbine with multisine signals and directly estimating linear engine models in the frequency domain. The paper noted that both noise and nonlinearities would influence the estimated models but did not present a detailed analysis of these effects, or attempt to quantify their influence. These sources of error are dealt with in detail in this paper and techniques proposed by which they can be analysed. All the approaches described rely on the use of periodic test signals to excite the engine and the data analysis and model estimation are conducted in the frequency-domain.

The overall aim of the work described was to estimate linear engine models at a series of operating points, in order to verify the linearised thermodynamic models of the engine. Thermodynamic models are derived during the development stage of an engine, based on knowledge of the engine physics, and provide important insights into the engine behaviour. Since these models are based on *a priori* assumptions about the engine physics it is then important to validate their performance against real engine data.

It was shown in the previous paper that frequency-domain identification techniques were well suited to this problem. A range of models were estimated and used to verify the thermodynamic models. They showed that, in the case of the particular engine tested, the thermodynamic models did not adequately represent the engine dynamics at higher operating points.

Since the aim is to verify the thermodynamic models using models estimated from engine data, it is very important to assess the possible sources of error on these estimated models. Three possible sources of error are discussed in this paper: noise, nonlinearities and unmodelled linear dynamics.

Following an introductory section presenting the key aspects of the frequency-domain approach, each of the sources of error will be dealt with in turn. All the techniques proposed are illustrated using practical results obtained using real engine data.

Presented at the International Gas Turbine & Aeroengine Congress & Exhibition
Indianapolis, Indiana — June 7–June 10, 1999

2. GAS TURBINE TESTING AND MODELLING

The engine tested in this work was a Rolls Royce Spey Mk 202, which is a typical military twin-shaft turbofan, with a low by-pass ratio and a variable reheat nozzle. The work concentrated on the dynamic relationship between the measured input fuel flow and the *high pressure* (HP) and *low pressure* (LP) shaft speeds, denoted *NH* and *NL*.

During the tests, the engine speed control was operated in open loop and a perturbed fuel demand signal fed to the fuel feed system, which regulates the fuel flow to the engine by means of a stepper valve. The fuel flow was measured downstream of the fuel feed system, using a turbine flow meter, in order to exclude the fuel feed dynamics from the engine model.

Multisine signals were used to excite the gas turbine, which are simply an arbitrary sum of harmonically related cosines

$$u(t) = \sum_{K=1}^{F} a_K \cos(i_K 2\pi f_0 t + \phi_K) \tag{1}$$

with **a** a vector of amplitudes, **i** a vector of harmonic numbers, f_0 the signal fundamental frequency and Φ a vector of phases. The harmonic phases must be carefully selected to minimise the crest factor of the signal, which is the ratio of its maximum absolute value to its root-mean-square value. The technique proposed by Guillaume *et al.* (1991) was employed, since it results in the lowest crest factors achieved to date.

The use of broad-band multisines allows a large number of frequency points to be measured in one test, which is much faster than measuring frequency-by-frequency using single sines. The advantage of multisines over binary signals is that their harmonic content can be arbitrarily defined. Two specific signals will be discussed in this paper. Firstly, an odd-harmonic multisine, from which all even harmonics have been excluded

$$\text{Odd} \qquad \mathbf{i} = [1 \quad 3 \quad 5 \quad 7 \quad 9 \quad \ldots \quad 59] \tag{2}$$

and secondly, a signal termed an odd-odd multisine, from which every other odd harmonic has also been excluded.

$$\text{Odd-Odd} \qquad \mathbf{i} = [1 \quad 5 \quad 9 \quad 13 \quad 17 \quad \ldots \quad 59] \tag{3}$$

The signal fundamental frequencies were set at 0.01 Hz, giving bandwidths of 0.01Hz-0.59Hz, in each case. This adequately covered the breakpoint frequencies of the shaft dynamics, based on an analysis of the thermodynamic models. Six periods of each signal were recorded in the tests, at a sampling frequency of 5 Hz. This gave 500 samples per signal period and total record lengths of 3000 samples per signal.

The data obtained from testing with multisine signals were then used to estimate both nonparametric and parametric models in the frequency-domain. Since periodic signals were used, the *frequency response function* (FRF) was estimated as the ratio of the mean values of the output and input Fourier coefficients, at the discrete test frequencies ω_K

$$\hat{H}_{EV}(j\omega_K) = \frac{\frac{1}{M}\sum_{m=1}^{M} Y_m(j\omega_K)}{\frac{1}{M}\sum_{m=1}^{M} U_m(j\omega_K)} = \frac{\overline{Y}(j\omega_K)}{\overline{U}(j\omega_K)} \tag{4}$$

where $U_M(j\omega_K)$ and $Y_M(j\omega_K)$ are the input and output spectra, measured across M periods of the input and output signals. This was termed the *error-in-variables* estimator by Guillaume (1992), who showed that it is both asymptotically unbiased and efficient in the presence of normally distributed noise on the real and imaginary parts of the input and output Fourier coefficients.

It is also important to consider the uncertainty of the FRF estimates. Schoukens *et al.* (1993) have shown that, using linear approximations, the estimator described above has the uncertainty

$$\sigma_H^2(\omega_k) = \frac{2}{M\,|\,U(j\omega_k)\,|^2}\left(\,|\,H(j\omega)\,|^2\,\sigma_U^2(\omega_k) + \sigma_Y^2(\omega_k) - 2\Re\{\,\sigma_{UY}(j\omega_k)H^*(j\omega_k)\,\}\right) \tag{5}$$

where the terms $\sigma_U^2(\omega_k)$ and $\sigma_Y^2(\omega_k)$ are the variances of the real or imaginary parts of the input and output noise and where $\sigma_{UY}(j\omega_k)$ is their cross-covariance. Correlated noise may be the result of input noise passing through the system or of the system operating within a feedback loop. It can be seen from equation (5) that the variance of the estimated FRF is inversely proportional to the number of measurements and the power of the input harmonics and directly proportional to the noise variances, referred to the system output.

Parametric frequency-domain identification involves selecting the parameters of an *s*-domain model

$$H(s) = \frac{b_0 + b_1 s + \ldots b_{nb}s^{nb}}{a_0 + a_1 s + \ldots a_{na}s^{na}} \exp(-sT_D) = \frac{N(s)}{D(s)} \exp(-sT_D) \tag{6}$$

where *nb* is the number of zeros, *na* is the number of poles and T_D is the pure time delay. Under the assumption of noise on both the input and output signals, Schoukens *et al.* (1988) derived an estimator of $H(s)$, which was subsequently developed by Pintelon *et al.* (1992), to arrive at a cost function

$$V(\mathbf{p}) = \frac{1}{2}\sum_{K=1}^{F} \frac{|\exp(-j\omega_K T_D)\,N(j\omega_K,\mathbf{p})\overline{U}(j\omega_K) - D(j\omega_K,\mathbf{p})\overline{Y}(j\omega_K)\,|^2}{\sigma_U^2(\omega_K,\mathbf{p}) + \sigma_Y^2(\omega_K,\mathbf{p}) - \sigma_{UY}(\omega_K,\mathbf{p})} \tag{7}$$

where the terms $\sigma_U^2(\omega_K,\mathbf{p})$ and $\sigma_Y^2(\omega_K,\mathbf{p})$ are proportional to the variances of the input and output noises and the term $\sigma_{UY}(\omega_K,\mathbf{p})$ is proportional to their covariance. The summation is across the number of frequency points F and $\mathbf{p}$ is a vector of the model parameters. If there are no modelling errors, the expected value of the cost function will be

$$V_{MIN} = F - \frac{np}{2} \tag{8}$$

As previously stated, the main aim of this work was to verify the linearised thermodynamic models of the engine. Jackson (1988) showed that, for a given stationary operating point, the higher-order nonlinear thermodynamic models derived from the engine physics can be reduced to linear models with the same order as the number of engine shafts. The linearised models are expressed in a state space form and the shaft speeds selected as the states, which is convenient since they can be directly measured. Evaluating the transfer function matrices of these models allows the HP and LP shaft dynamics to be expressed in transfer function form, with common poles but different zeros.

The linearised models obtained are second order, with real poles and zeros. The HP shaft has a cancelling pole-zero pair for most of the operating range, reducing the model to first order. The pole and zero of th LP shaft are more distinct.

The poles and zeros of the linearised thermodynamic models, along with the estimated first-order HP shaft and second-order LP shaft models, are plotted in Fig. 1. This was the final figure of the previous paper (Evans, 1998) and illustrates the variation of the pole and zero positions with operating point. It is clear from these results that the thermodynamic models are not adequately representing the dynamics of either shaft at higher operating points and that the second-order dynamics of the LP shaft are also badly represented. These second-order dynamics are of particular interest since they model the interaction between the shafts.

In order to have complete confidence in the estimated linear models it is necessary to conduct a thorough assessment of the possible sources of error in the measured data and their influence on the estimated models. Such an analysis will now be conducted for each source of error in turn.

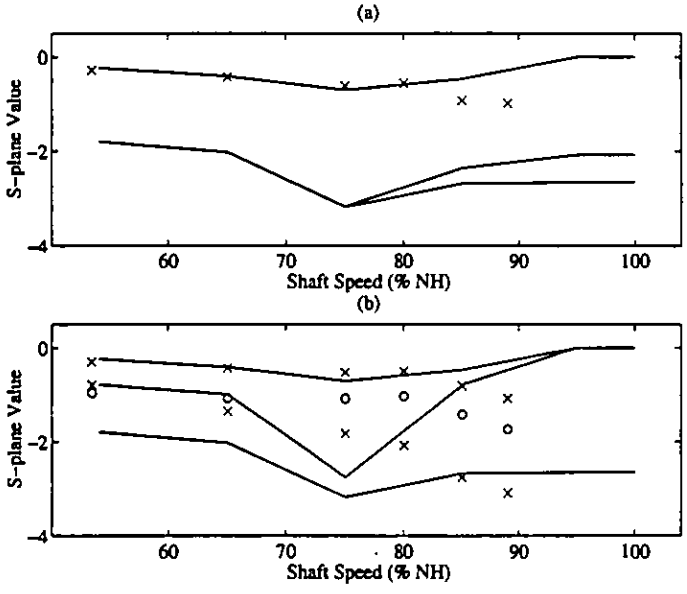

Figure 1. Variation of engine models for (a) HP shaft and (b) LP shaft. Estimated models shown as poles (x) and zeros (o) and thermodynamic models as poles (solid) and zeros (dashed).

3. NOISE

A first indication of the noise levels present in the data can be obtained by transforming the complete data lengths into the frequency-domain using the FFT. Since the frequency resolution of the FFT is inversely proportional to the total time of the data record ($\Delta f = 1/T_{TEST}$), this will give the greatest resolution achievable with those data. A plot of the input spectrum and the HP shaft output spectrum for the odd-odd multisine is shown in Fig 3. It is then possible to calculate the total power in the signal P_{TOT}, and the power at the excited harmonics P_{TEST}. An initial estimate of the signal-to-noise ratio (SNR) can then be obtained by treating all the power at nonexcited frequencies as noise

$$SNR_{TD} = 10 \log_{10}\left(\frac{P_{TEST}}{P_{TOT} - P_{TEST}}\right) \tag{9}$$

This is a measure of the total excitation power over the total remaining power and is hence a calculation of the raw time-domain SNR, which can be improved by further processing.

The next step in the noise analysis is to estimate the sample means, variances and covariance of the excited input and output Fourier coefficients, which are needed both to estimate the uncertainty on the FRF estimates and as *a priori* information for the parametric frequency-domain estimator. For this purpose, the data must be transformed to the frequency domain on a period-by-period basis. The following estimates can then be made

$$\overline{V}(j\omega_k) = \frac{1}{M}\sum_{m=1}^{M} V_m(j\omega_k) \tag{10}$$

$$\sigma_V^2(\omega_k) = \frac{1}{M-1}\sum_{m=1}^{M}\left(V_m(j\omega_k) - \overline{V}(j\omega_k)\right)\left(V_m(j\omega_k) - \overline{V}(j\omega_k)\right)^* \tag{11}$$

where $V(j\omega_k)$ is interchangeably $U(j\omega_k)$ or $Y(j\omega_k)$. Since the Fourier coefficients are complex the variance calculated according to equation (11) will be the sum of the variances of the real and imaginary parts. The covariance can be estimated as

$$\sigma_{UY}(j\omega_k) = \frac{1}{M-1}\sum_{m=1}^{M}\left(\left(U_m(j\omega_k) - \overline{U}(j\omega_k)\right)\left(\left(Y_m(j\omega_k) - \overline{Y}(j\omega_k)\right)\right)\right) \tag{12}$$

A significant covariance indicates that the input noise is not simply present in the input measurement channel but also passes through the system and is hence correlated with the output noise. The variances and covariance calculated in this way are double the quantities required for equations (5) and (7), where the variances and covariance of the real or imaginary parts are used.

Since the estimation will be conducted only at the excited frequencies it is now possible to exclude all the other frequency points, which are termed *noise lines*, from the data. Assuming the presence of stationary white noise, the improvement in SNR will be in the order of

$$SNR_{EX} = SNR_{TD} + 10 \log_{10}\left(\frac{N}{2F}\right) \tag{13}$$

where N is the number of samples per period and the improvement depends on the degree of over-sampling employed. Since the means and variances estimated from equations (10) and (11) are a measure of the periodic and stochastic power, respectively, they can be used to calculate the actual SNR following the exclusion of the noise lines

$$SNR_{VEX} = 10 \log_{10}\left(\frac{\sum_{k=1}^{F} |\overline{V}(j\omega_k)|^2}{\sum_{k=1}^{F} \sigma_V^2(\omega_k)}\right) \tag{14}$$

A further improvement in the SNRs is provided by averaging the data across M periods. The variance of the sample means is smaller than the sample variances estimated using equation (11), by a factor of $1/M$. This will provide a further improvement in the SNR of

$$SNR_{VAV} = SNR_{VEX} + 10 \log_{10}(M) \tag{15}$$

Six signal periods were measured during each test at an amplitude of ±10% of the steady-state fuel feed (W_F) and the means, variances and covariance were estimated as described above. The variances and covariance are plotted for the 30 odd harmonic HP shaft data in Figure 2, which shows stronger noise variance at low frequency and also a larger covariance at those frequencies. The significant covariance is to be expected since the dominant noise source at the input is turbulence in the fuel flow, which also passes through the system and is hence correlated with the output noise.

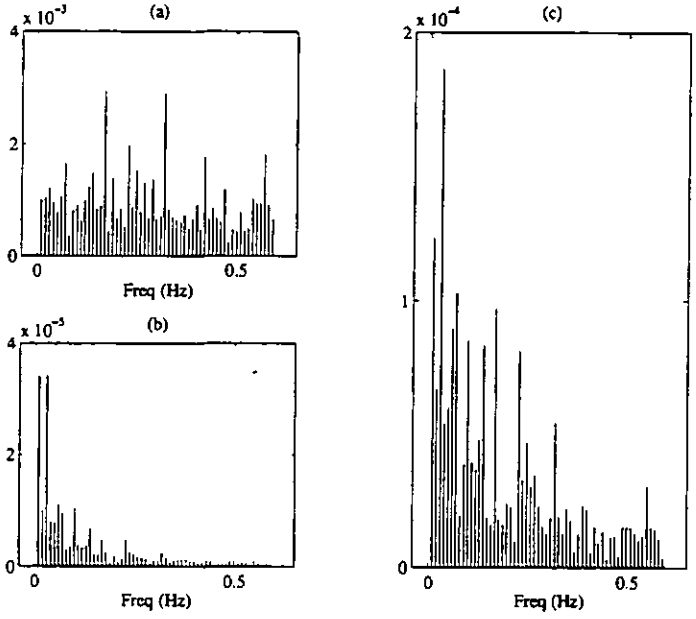

Figure 2. Noise variances on (a) input and (b) output, and (c) absolute value of covariance, for 30 odd harmonic signal, HP shaft.

The SNRs were also calculated, beginning with an estimate of the raw time-domain SNR using equation (9). The improved SNRs achieved by excluding the noise lines and by averaging over six periods were then calculated using equations (14) and (15) and the results are shown in Table 1.

The SNRs after averaging are very good, with values of at least 40 dB in each case. According to equation (13) the exclusion of the noise lines should have improved the time-domain SNRs by around 9 dB, ($10.\log_{10}(500/60)$), for the odd harmonic signal, and 12 dB for the odd-odd signal. An improvement of this order was obtained for the input frequencies but the improvement was not as great for the outputs, since the output noise is not white and its power is concentrated in the test signal bandwidth. Given such high SNRs the influence of noise on the models estimated with these data will be very small.

TABLE 1

SIGNAL-TO-NOISE RATIOS

	30 Odd Harmonics			15 Odd-odd Harmonics		
SNR (dB)	Input	HP	LP	Input	HP	LP
Time domain	24	29	27	23	28	26
Excluding noise lines	33	34	34	43	44	44
Averaging	40	42	42	51	52	52

4. NONLINEARITIES

Before proceeding with testing and identification it is necessary to establish whether the system can be considered linear across the specified time-domain input amplitude. There are a variety of techniques for establishing the linearity of a system, the simplest being to inject a series of single sinewaves of increasing amplitude and look for distortion of the output signal (Haber, 1985).

Some idea of the system bandwidth is also required in order to properly design the test signals for linear identification. This can be achieved by injecting a wide band pilot test signal. However, time is usually at a premium when testing industrial systems, due to operational or financial constraints. It is therefore desirable to minimise the time spent on initial tests by combining these two operations. This can be achieved by using a wide-band multisine, with certain harmonics excluded, as the pilot signal.

If all the even harmonics and some of the odd harmonics are excluded from the signal then nonlinear effects can be detected by the presence of harmonics between the test frequencies in the output. By using an odd-odd multisine, with the harmonic vector shown in equation (3), the harmonics generated by even and odd-order nonlinearities will fall at even and odd omitted harmonics, respectively. It is thus possible to classify the output contributions as arising from even nr odd nonlinearities.

A criterion is required to assess whether any of the additional output components are indeed periodic nonlinear contributions, or simply noise harmonics. McCormack *et al.* (1995) proposed using the squared coherence function, defined for systems with a noise free input, which depends only on the output signal

$$\gamma_{ni}^2(\omega) = \frac{|\frac{1}{M}\sum_{m=1}^{M} Y_m(j\omega)|^2}{\frac{1}{M}\sum_{m=1}^{M} Y_m(j\omega)Y_m^*(j\omega)} = \frac{|\overline{Y}(j\omega)|^2}{G_{YY}(\omega)} \tag{16}$$

where $Y_m(j\omega)$ is the output spectrum at the excited and nonexcited frequencies, measured across M periods and $G_{YY}(\omega)$ is the auto-covariance (power spectrum) of that signal. The quantity $\gamma_{ni}^2(\omega)$ is termed the *nonlinear coherence* to distinguish it from the more commonly used definition of coherence. Assuming the presence of uncorrelated input and output noise then equation (16) can be expressed as

$$\gamma_{ni}^2(\omega) = \frac{G_{YY}(\omega) + (G_{NN}(\omega)/M)}{G_{YY}(\omega) + G_{NN}(\omega)} \tag{17}$$

where $G_{NN}(\omega)$ is the auto-covariance of the output noise. This shows that, as M becomes large, the nonlinear coherence will express the ratio of the periodic power over the total power at each output frequency. If the periodic component is zero, it will assume a value of $1/M$, which gives an useful bound with which to judge the significance of the nonlinear coherence values. It can be assumed that all those values which lie close to this bound are simply a function of noise and do not indicate the presence of any periodic nonlinear contributions.

The presence of nonlinearities was investigated by examining the FFT of the odd-odd signal at the input and HP shaft output, shown in Figure 3. There appear to be some excluded even harmonics rising above the noise floor on the output but it is difficult to conclude that these are indeed periodic nonlinear contributions.

A clearer picture is obtained from the nonlinear coherence, calculated using equation (16), which is plotted in Figure 4 for the excluded odd and even harmonics. Since six signal periods were measured the $1/M$ bound is 0.17 in this case. It can be seen that only one frequency has a significant coherence in the input spectrum, within the signal bandwidth, while a series of even harmonics have a significant coherence in the output. The odd coherence is consistently much lower on both the input and output. This suggests that the fuel feed can be considered as linear over this range, while a weak even-order nonlinearity may be present in the gas turbine. A similar result was obtained with the LP shaft which suggests that it will be possible to eliminate the influence of nonlinearities on the estimated linear model simply by using an odd harmonic signal.

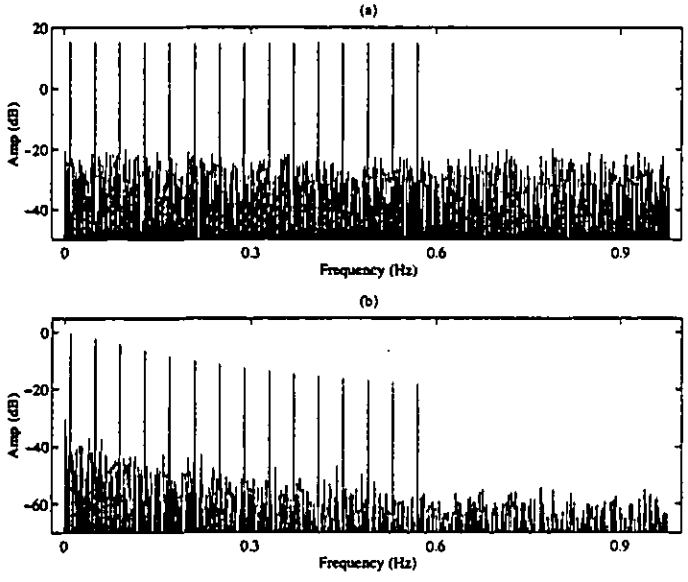

Figure 3. Odd-odd multisine spectrum at (a) input and (b) HP shaft output.

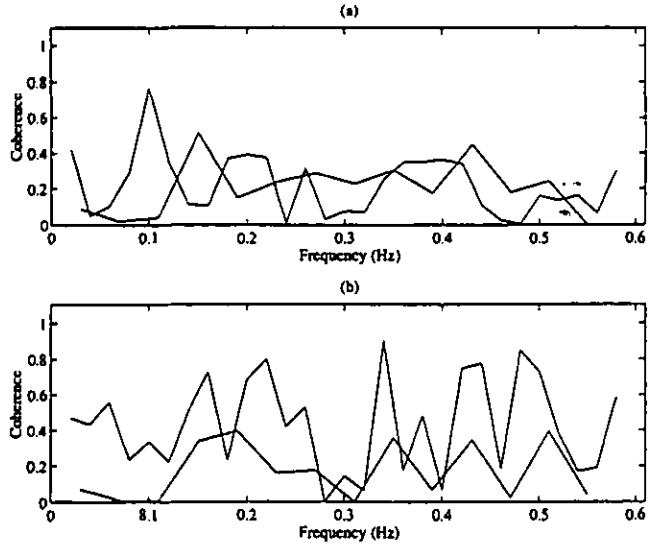

Figure 4. Nonlinear coherence of odd-odd multisine at (a) input and (b) HP shaft output. Showing excluded even harmonics (solid) and odd harmonics (dashed).

Using the odd multisine data for linear estimation should therefore give high quality estimates of the engine dynamics, unaffected by nonlinearities. In practice, it was not possible to apply a pure odd signal to the gas turbine, since process noise was present at the engine input. This meant that the input signal had small amounts of power at the even harmonics, which would interact with the even nonlinearity to create distortion at the odd excitation harmonics. Since the input SNR was high and the nonlinear influence was very low it was expected that this effect would be negligible.

Thus the techniques revealed the presence of a weak even-order nonlinear effect in the engine, for an input amplitude of $\pm 10\%$ W_f. This nonlinearity did not have any influence on the test signals used, since they were composed of only odd-harmonics and hence all even-order nonlinear contributions will fall at even output harmonics. Using the odd multisine data for linear estimation will thus give high quality estimates of the engine dynamics, unaffected by nonlinearities.

5. UNMODELLED LINEAR DYNAMICS

The main aim of the current work was to study the shaft dynamics of the engine and the test signal bandwidths were selected accordingly. However, dynamics outside the frequency range of the test signals can have an influence on the data and introduce bias into the shaft speed models. It is therefore important to assess the influence of any unmodelled linear dynamics. This will now be studied by examining the evolution of the shaft speed models with increased model order and also by progressively excluding frequencies from the estimation data set.

Table 2 shows models of increasing order for the HP shaft, along with the estimator cost function. The major drop in the cost function occurs with the one zero, two pole (1/2) model, suggesting that this is the best structure. The table also shows the pole and zero positions of these models, with their standard deviations expressed as a percentage of their magnitudes. The 1/2 model has a pole-zero pair close to the origin, whose 2σ regions of uncertainty do, however, overlap. Adding another pole and zero gives an unstable pole, which is not a credible model.

TABLE 2
ESTIMATION RESULTS FOR HP SHAFT

Order	Cost Function	Zeros	σ_z (%)	Poles	σ_p (%)
0/1	280	—	—	-0.5015	0.2
1/2	34	-0.3405	9.2	-0.2749 -0.6017	7.3 2.4
2/3	32	-0.3606 -19.640	11 64	-0.2860 -0.6145 16.336	8.1 3.6 39

The variation of the cost function for the LP shaft models, estimated using the 30 odd harmonic data, is presented in Table 3. The large drop in the cost function between the 0/1 and 1/2 models shows that the dynamics are at least second-order. There is even a case for selecting a 2/3 model, though the drop in the cost function is not as significant as that for the 1/2 model.

The table shows that the 2/3 model has a very close pole-zero pair near the origin, the uncertainty regions of which do overlap. This close pole-zero pair is once again modelling a low frequency effect in a similar way to the pole-zero pair in the 1/2 model of the HP shaft.

TABLE 3

ESTIMATION RESULTS FOR LP SHAFT

Order	Cost Function	Zeros	σ_z (%)	Poles	σ_p (%)
0/1	4609	—	—	-0.7939	0.2
1/2	69	-0.9064	2.2	-0.4199	1.2
				-1.8250	1.7
2/3	39.55	-0.1127	31	-0.1042	30
		-1.0496	3.9	-0.4754	3.3
				-1.9783	2.6
3/4	39.54	-0.1156	31	-0.1068	30
		-1.0533	4.1	-0.4768	3.4
		1.5033	28	1.5026	28
				-1.9831	2.7

It is clear that the HP and LP shafts have different order dynamics, with the HP shaft being predominantly first-order and the LP shaft second-order. In each case, the addition of a further pole-zero pair models a low frequency effect and significantly reduces the model cost function.

The influence of this low frequency mode on the estimated models can be assessed by excluding a number of the lower harmonics from the data set, re-estimating a range of models and monitoring the drop in the cost function as the model order is increased. This approach was applied to the 30 odd harmonic data for the HP shaft, with the lowest four, eight and then 12 harmonics progressively excluded from the data. The resulting drop in the cost function between the 0/1 and 1/2 models is shown in Table 4 and the influence on the estimated pole and zero positions shown in Table 5.

The role of the pole-zero pair in modelling a low frequency mode is clearly illustrated, since there is little benefit in increasing the model order to 1/2 once eight or more harmonics have been omitted from the data. Omitting harmonics has little influence on the estimate of the dominant pole but has a significant influence on the pole-zero pair. A similar pattern was observed for the transition between the 1/2 and 2/3 models of the LP shaft.

Hence if a model is required that adequately describes the HP shaft speed dynamics in the frequency range 0.17 Hz - 0.59 Hz then the 0/1 structure will be sufficient. If a model is required which covers the complete frequency range of the test signals then the additional pole-zero pair should be included. Models can be estimated for selected frequency ranges in both the time and frequency domains but the ease with which this can be achieved in the frequency-domain is an attractive feature of this approach.

TABLE 4

VARIATION OF COST FUNCTION WITH OMITTED FREQUENCIES

Omitted Frequencies	f_{min} (Hz)	Cost Function (K)	
		0/1 Model	1/2 Model
0	0.01	280	34
4	0.09	66	26
8	0.17	21.2	19.9
12	0.25	15.4	15.0

TABLE 5

VARIATION OF ESTIMATED MODELS WITH OMITTED FREQUENCIES

Omitted Frequencies	Zero	Pole 1	Pole 2
0	-0.3405	-0.2749	-0.6017
4	-0.3664	-0.2904	-0.6163
8	-0.5076	-0.4090	-0.6456
12	-51440	-34.29	-0.5423

6. CONCLUSIONS

The frequency-domain identification of the fuel flow to shaft speed dynamics of a twin-shaft gas turbine has been studied with the aim of assessing the accuracy of the estimates in the presence of noise, nonlinear effects and the unmodelled system dynamics.

The frequency-domain noise analysis revealed significant correlation between the input and the output noise, particularly at low frequency. The frequency-domain SNRs after averaging and excluding the noise lines were 40db or better at the input and the outputs. Such high SNRs mean that the noise present on the measurements will have a negligible influence on the estimated models.

The presence of nonlinear effects was investigated by calculating the nonlinear coherence of the odd-odd multisine at the unexcited frequencies. This showed the fuel feed system to be linear, for the input amplitude employed, with a weak even-order nonlinearity present in the engine.

The presence of a weak even-power engine nonlinearity did not influence the test frequencies due to the use of odd-harmonic signals. It was thus possible to use frequency-domain techniques to estimate linear engine models which were free from the influence of any significant nonlinear effects. It can thus be stated with some confidence that the small signal dynamics of the shafts have been accurately identified.

Additional low frequency effects were detected on both shafts which could be modelled by the addition of a close pole-zero pair. The influence of these low frequency modes was studied by excluding the lower frequencies from the data set and re-estimating a range of models. The time constants of the additional pole-zero pairs are too slow to be associated with the shaft dynamics which suggests that they may be modelling thermal effects, which are not incorporated in the thermodynamic models.

Acknowledgments

This work was conducted with the support of Rolls Royce plc and the UK Defence Evaluation and Research Agency at Pyestock. The authors would like to thank all the staff involved. Thanks also to Neophytos Chiras for his help in preparing this paper.

REFERENCES

Evans, C., Borrell, A. and D. Rees (1998). "Testing and modelling gas turbines using multisine signals and frequency-domain techniques", *ASME Gas Turbine Conference*, paper 98-GT-98, pp. 1-8.

Guillaume, P., J. Schoukens, R. Pintelon and I. Kollár (1991). "Crest factor minimisation using nonlinear Chebyshev approximation methods", *IEEE Trans. Instrumentation and Measurement*, vol. 40, no. 6, pp. 982-989.

Guillaume, P. (1992). *Identification of multi-input multi-output systems using frequency-domain methods*, Ph.D. Thesis, Vrije Universiteit Brussel, Department ELEC, Brussels.

Haber, R. (1985). "Nonlinearity tests for dynamic processes", in *Proc. 7th IFAC Symposium on Identification and System Parameter Estimation*, York, pp. 409-414.

Jackson, D. (1988). "Investigation of state space architectures for engine models", *Rolls Royce plc*, Report TDR 9331.

McCormack, A.S., K.R. Godfrey and J.O. Flower (1995). "The design of multilevel multiharmonic signals for system identification", *IEE Proc. Control Theory and Applications*, vol. 142, no. 3, pp. 247-252.

Pintelon, R., P. Guillaume, Y. Rolain and F. Verbeyst (1992). "Identification of linear systems captured in a feedback loop", *IEEE Trans. Instrumentation and Measurement*, vol. 41, no. 6, pp 747-754.

Schoukens, J., R. Pintelon and J. Renneboog (1988). "A maximum likelihood estimator for linear and nonlinear systems - a practical application of estimation techniques in measurement problems", *IEEE Trans. Instrumentation and Measurement*, vol. 37, pp. 10-17.

Schoukens, J., P. Guillaume and R. Pintelon (1993). "Design of broadband excitation signals", chapter 3 of *Perturbation Signals for System Identification*, K. Godfrey (ed.), Prentice Hall, New York.